



NOAA Technical Memorandum OAR ARL-279  
<https://doi.org/10.25923/a5kx-ap26>

# Improved Sampling of the Atmospheric Boundary Layer Using Small Unmanned Aircraft Systems: Results from the Avon Park Experiment

---

Temple R. Lee  
Edward Dumas  
Michael S. Buban  
C. Bruce Baker  
Jonathan Neuhaus  
Mark Rogers  
Nicole Chappelle  
Casey Marwine  
Maureen Swanson  
Chris Amaral  
Phillip Hall

May 2019

National Oceanic and Atmospheric Administration  
Oceanic and Atmospheric Research  
Air Resources Laboratory  
Atmospheric Turbulence and Diffusion Division  
Oak Ridge, Tennessee



NOAA Technical Memorandum OAR ARL-279  
<https://doi.org/10.25923/a5kx-ap26>

## Improved Sampling of the Atmospheric Boundary Layer Using Small Unmanned Aircraft Systems: Results from the Avon Park Experiment

*By Temple R. Lee, Edward Dumas, Michael S. Buban, C. Bruce Baker,  
Jonathan Neuhaus, Mark Rogers, Nicole Chappelle, Casey Marwine,  
Maureen Swanson, Chris Amaral, Phillip Hall*

May 2019

National Oceanic and Atmospheric Administration  
Oceanic and Atmospheric Research  
Air Resources Laboratory  
Atmospheric Turbulence and Diffusion Division  
Oak Ridge, Tennessee

U.S. Department of Commerce  
Secretary of Commerce Wilbur Ross

Under Secretary for Oceans and Atmosphere/Acting NOAA Administrator  
Dr. Neil Jacobs

Assistant Secretary for Oceans and Atmosphere/Deputy NOAA Administrator  
RDML Tim Gallaudet, Ph.D., USN Ret.

## **Abstract**

Earth's atmospheric boundary layer (ABL) has traditionally been difficult to sample, yet adequate characterizations of it are essential to weather forecasting. In recent years, small unmanned aircraft systems (sUASs) have begun to be used to sample the ABL. Current regulations allow for sUAS to be operated by NOAA within visual line-of-sight (VLOS) up to 365 m (1200 ft) above ground level (AGL) outside of five nautical miles from airports. However, obtaining information above 1200 ft AGL is essential if sUAS are to be used to support weather forecasting operations. Transitioning sUAS into forecast operations will also require operating sUAS beyond visual line of site (BLVOS). To support this effort, scientists and engineers from the NOAA Air Resources Laboratory (ARL) Atmospheric Turbulence and Diffusion Division (ATDD) conducted an experiment on 4-6 March 2019 near Avon Park, FL with two of its sUAS: a Meteomatics Meteodrone SSE and a BlackSwift Technologies S2. The team also deployed a ground-based radar system integrated with geospatial software to determine its ability to mitigate potential threats to the sUASs by targets within the airspace. During the testing period, the team performed 17 flights with the Meteodrone and 7 flights with the S2. During all tests, the ground-based radar system was able to detect both the Meteodrone and S2, as well as other air traffic in the area. Overall, this experiment was an important step towards operation of sUAS to higher altitudes to ultimately allow them to support operational weather forecasting.

## **1. Introduction**

Earth's atmospheric boundary layer (ABL) has traditionally been difficult to sample, yet adequate characterizations of it are essential to weather forecasting. Surface-based observational

platforms, e.g., weather stations and flux towers, penetrate at most a few tens of meters into the ABL (Figure 1). Rawinsondes provide only a snapshot of the ABL and are generally released only twice daily from locations that are unevenly distributed across the world. Like rawinsondes, surface-based lidars and sodars provide profiles at only one dimension in space, but also have more limited vertical resolution (Wulfmeyer et al. 2016, Lundquist et al. 2017). Although radars provide better spatial coverage than rawinsondes, lidars, and sodars, oftentimes radars overshoot the ABL and therefore do not sample it well.

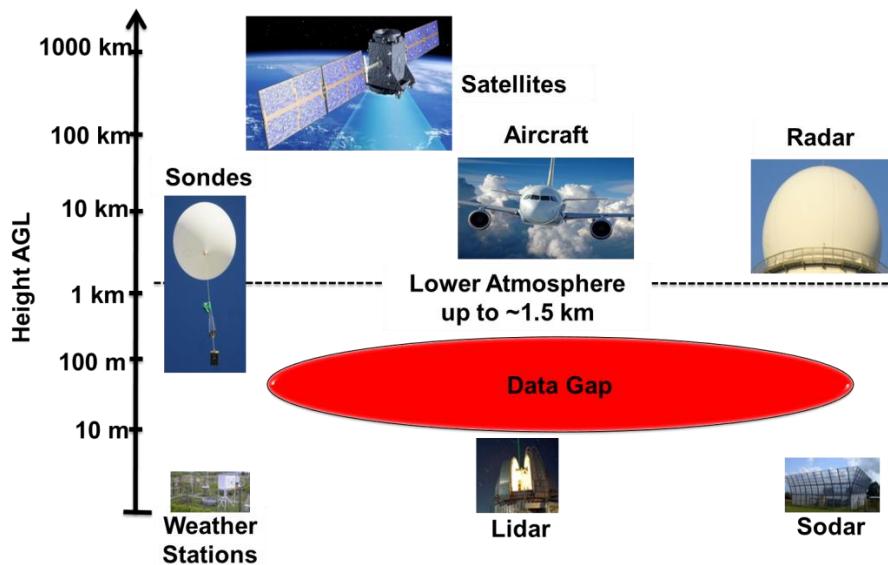


**Figure 1:** Observational data gap in the atmosphere for which sUAS can be used to improve sampling.

Small unmanned aircraft systems (sUAS) have the potential to help close this significant observation gap. As summarized in Lee et al. (2019), closing this gap is essential for a myriad of weather forecasting applications. Knowledge of near-surface thermodynamic characteristics is essential for determining winter precipitation type (e.g., Bourgoïn et al., 2000, Thériault et al. 2006), and forecasting the strength of the elevated capping inversion atop the ABL is critical for forecasting convection initiation (e.g., Hardesty and Hoff 2012). Additionally, sUAS

observations can be assimilated into numerical weather prediction (NWP) models (Jonassen et al. 2012, Ágústsson et al. 2014, Flagg et al. 2018) to improve weather forecasts, and used as initial and boundary conditions in idealized simulations to improve NWP model physics.

Making measurements using sUAS, though, requires obtaining the necessary permissions from the Federal Aviation Administration (FAA). Current regulations allow NOAA to operate sUAS within visual line-of-sight (VLOS) up to 365 m (1200 ft) above ground level (AGL) in Class G airspace. Obtaining atmospheric thermodynamic and kinematic information within the lowest few hundred meters of the atmosphere has so far proven useful for a variety of research applications in the atmospheric sciences. These applications include characterizations of the spatio-temporal variability in low-level temperature and moisture fields during recent field studies (Lee et al. 2019a), deriving horizontal-scale variability in surface sensible heat flux surrounding micrometeorological towers (Lee et al. 2017), and studying the response of the land surface and lower ABL during the Great American eclipse of 2017 (Lee et al. 2018, Buban et al., 2019).

However, obtaining information above 365 m AGL and sampling within and above the planetary boundary layer (PBL) (which can at times exceed 3000 m in depth) is essential if sUAS are to be used to support weather forecasting operations. Making this transition requires operating sUAS beyond visual line of site (BLVOS). When operating sUAS using BVLOS, the sUAS pilot must be aware of other aircraft in the sUAS' airspace in order to take appropriate deconfliction decisions. Information on other aircraft operating in the vicinity requires the use of ground-based detect-and-avoid (DAA) radar systems, as well as real-time information on air traffic.

## 2. Experimental Design

To support the effort to transition sUAS to BVLOS, on 4-6 March 2019, a team of nine NOAA scientists and engineers conducted an experiment at Avon Park, a U.S. Air Force (USAF) test range north of Sebring, Florida (Figure 2), using two sUASs from the NOAA Air Resources Laboratory (ARL) Atmospheric Turbulence and Diffusion Division (ATDD). The team consisted of personnel from NOAA/ARL/ATDD, NOAA's Unmanned Aircraft Systems Program Office (UASPO), and NOAA's Office of Marine and Aviation Operations (OMAO) Aircraft Operations Center (AOC). The testing facility at Avon Park (27.65 °N, 81.34 °W, 20 m above mean sea level (MSL)) is located about 114 km southeast of Tampa and 100 km south of Orlando.



**Figure 2:** Location of Avon Park relative to Tampa and Orlando, FL.

The two sUASs tested were a Meteomatics Meteodrone SSE and a BlackSwift Technologies (BST) S2 fixed-wing aircraft (Figure 3). The Meteodrone SSE performs vertical takeoff and landings (VTOL) and is used to measure air temperature, moisture, and wind. The BST S2 is a fixed-wing aircraft equipped with sensors to measure air temperature, moisture, and pressure (accomplished using an International Met Systems XQ-2 sensor), and land surface

temperature using a downward-pointing TeAx ThermalFusion visible and infrared camera. Characteristics of these two sUAS are summarized in Table 1.

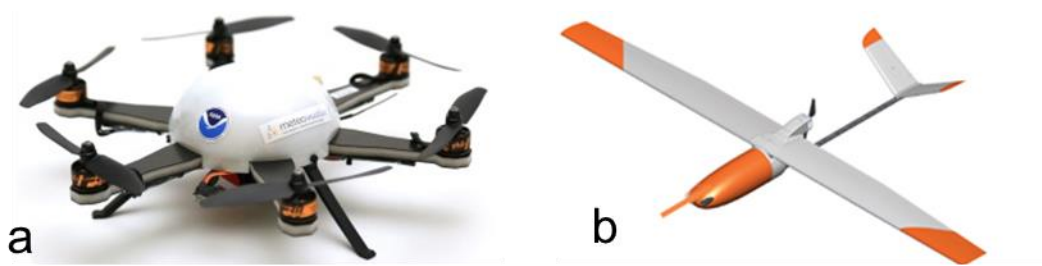


**Figure 3:** Meteomatics Meteodrone SSE (a) and BlackSwift Technologies S2 (b).

**Table 1:** Characteristics of the sUASs used in the study at Avon Park, FL, obtained from the respective manufacturers.

Model	Meteodrone SSE	BST S2
Registration Number(s)	FA3NEYLHN3	FA3PTCFHWM
Manufacturer	Meteodrone	BlackSwift Technologies
Units in Fleet	1	1 (1 pending)
Vehicle Type	Multi-rotor	Fixed-wing
Gross Weight	0.7 kg	6.6 kg
Wing Span	0.6 m	3.0 m
Length	0.6 m	2.0 m
Payload Capacity	--	2.3 kg
Engine Type	6 electric motors	1 electric motor
Autopilot	Meteodrone	SwiftPilot
Max Speed	19 m s <sup>-1</sup>	24.7 m s <sup>-1</sup>
Loiter Speed	0 m s <sup>-1</sup>	15 m s <sup>-1</sup>

Avon Park is a USAF bombing range which NOAA AOC has utilized to test both full-size and drone systems in the past. Because it is under Air Force control, its airspace is not subject to the same FAA restrictions that are imposed on the rest of the National Airspace System (NAS). These relaxed limitations enabled the NOAA team to fly both sUASs to their

respective maximum flight altitudes of ~ 1500 m (5000 ft) AGL. During testing, the team also deployed a ground-based radar system, manufactured by Echodyne, integrated with geospatial software produced by Kongsberg Geospatial Ltd. to determine its capability to mitigate potential threats to the sUASs by targets within the airspace (e.g., traditional airplanes, other sUASs, hot air balloons, birds, etc.).

Over the three-day testing period, the group performed 17 vertical profile flights with the Meteodrone SSE (Table 2) and 7 flights with the BST S2 (Table 3). The Meteodrone SSE performed solely VTOLs from the location shown in Figure 4 and was flown up to a maximum altitude of 950 m AGL during one of the flights. The BST S2 was launched from a site approximately 80 m east of the VTOL flights (c.f., Figure 4). On 4 and 5 March, the BST S2 was flown in a spiral, with a diameter of 100 m, up to an altitude of 1200 m AGL during one of the flights. The purpose of these flights was to compare data from the BST S2 with the Meteodrone SSE and to determine the maximum altitude to which the BST S2 is visible to the unaided eye. On 6 March, the BST S2 was flown in a series of lawnmower-type flights over the grassy fields located north and east of the takeoff location. The purpose of these flights was to characterize the spatial variability in air temperature, moisture, and also the thermal characteristics of the land surface.



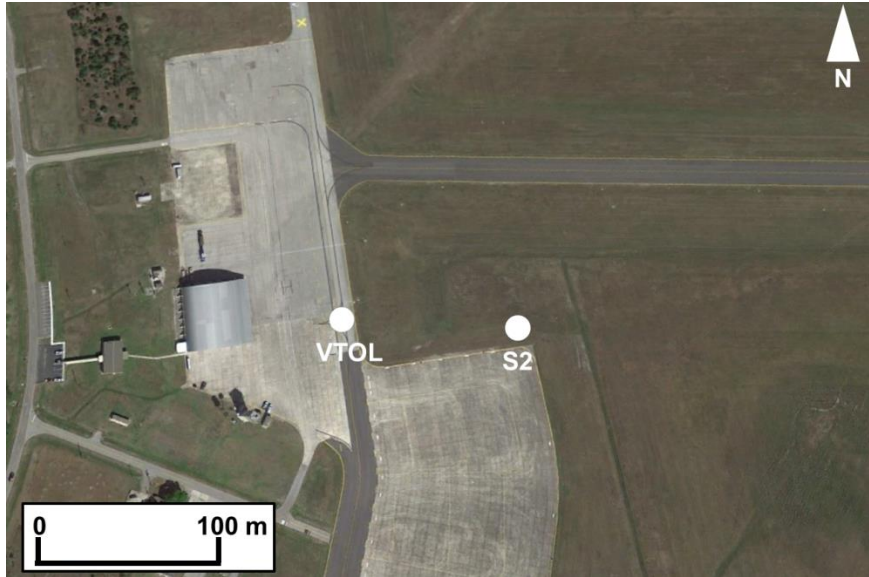


**Figure 4:** Relative locations of the Meteodrone SSE and BST S2 flights during the 4-6 March 2019 sUAS flights at Avon Park, FL.

**Table 2:** Start time and end time of the Meteodrone SSE sUAS flights. UTC = LST – 5.

<b>Date</b>	<b>Flight Number</b>	<b>Flight Start Time (UTC)</b>	<b>Flight End Time (UTC)</b>
4 Mar 2019	1	14:24	14:32
4 Mar 2019	2	15:12	15:18
4 Mar 2019	3	15:43	15:49
4 Mar 2019	4	16:05	16:10
5 Mar 2019	5	20:29	20:35
5 Mar 2019	6	20:43	20:49
6 Mar 2019	7	14:10	14:15
6 Mar 2019	8	14:22	14:27
6 Mar 2019	9	14:34	14:38
6 Mar 2019	10	14:42	14:47
6 Mar 2019	11	14:56	15:01
6 Mar 2019	12	20:23	20:28
6 Mar 2019	13	20:34	20:41
6 Mar 2019	14	20:46	20:53
6 Mar 2019	15	20:57	21:06
6 Mar 2019	16	21:10	21:17
6 Mar 2019	17	21:24	21:36

**Table 3:** Start time and end time of the BST S2 flights.

Date	Flight Number	Flight Start Time (UTC)	Flight End Time (UTC)
4 Mar 2019	1	19:14	19:28
4 Mar 2019	2	20:01	20:17
4 Mar 2019	3	20:32	20:59
5 Mar 2019	4	20:16	20:52
5 Mar 2019	5	21:08	21:59
6 Mar 2019	6	19:03	19:37
6 Mar 2019	7	20:32	21:07

### 3. Results

#### 3.1 Inter-comparison between BST S2 and Meteodrone SSE sUAS measurements

Prior to deployment at Avon Park, all thermodynamic sensors used on both sUAS were extensively characterized in ATDD’s National Institutes for Standards and Technology (NIST)-traceable calibration chambers and also through comparison of sensors used on sUASs with other meteorological platforms traditionally used for atmospheric observations (i.e., instrumented towers, other rawinsondes, etc.). More details on these inter-comparisons are summarized in Lee et al. (2019). To illustrate the agreement between the sensors used on the different platforms and to provide us with additional confidence in the fidelity of the measurements, air temperature and dew point temperature from the Meteodrone SSE were compared with data from the iMet-XQ2 on the BST S2, when the BST S2 was flown in a spiral (i.e., Flight 5 with the Meteodrone SSE and Flight 4 with the BST S2). The sensors on the Meteodrone SSE and BST S2 showed good agreement; temperatures agreed to  $\pm 0.2$  °C (Figure 5a), and dew point temperature was about 0.5 °C higher than the BST S2 (Figure 5b).

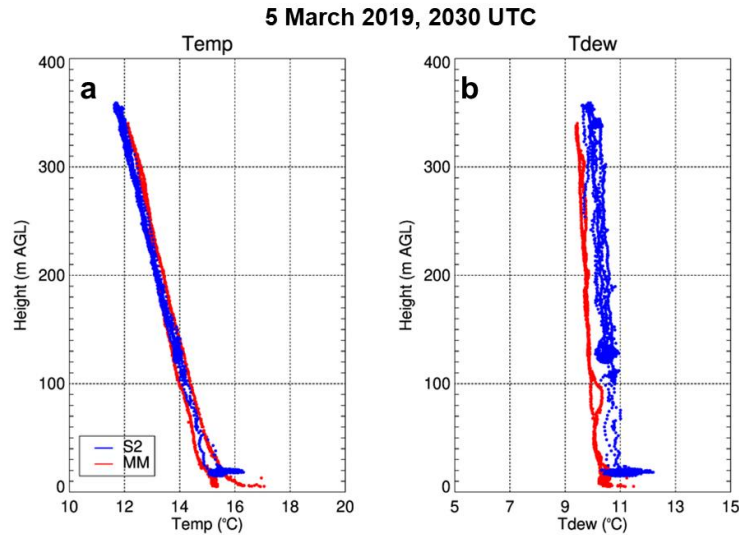


**Figure 5:** Temperature (a) and dew point temperature (b) from the BST S2 (blue) and Meteodrone SSE (red) sUAS at 20:30 UTC 5 Mar 2019.

### 3.2. Meteodrone SSE VTOL Profiles

Data from flights with the Meteodrone SSE were used to generate analyses of temperature, moisture, and wind fields, as well as a myriad of other derived meteorological quantities (e.g., refractivity, air density, estimates of sensible and latent heat flux, etc.) in near real-time using the Meteomatics software package. These profiles are illustrated using data from 6 March 2019, in which six flights were performed between 20:15 UTC and 21:30 UTC, up to a maximum altitude of 950 m during the final flight. During this 75 min period in the mid-afternoon, the vertical profiles show, e.g., the increasing destabilization of the lowest ~ 30 m of the PBL (Figure 6a, 6b), decrease in PBL moisture (Figure 6c), and increased mechanical mixing (Figure 6d). Over upcoming months, these same types of plots, as well as the corresponding quality-controlled data, will be generated in real-time and will be provided to local National

Weather Service (NWS) forecast offices to assist with weather forecasting decisions. More details on these plans appear in Section 4.

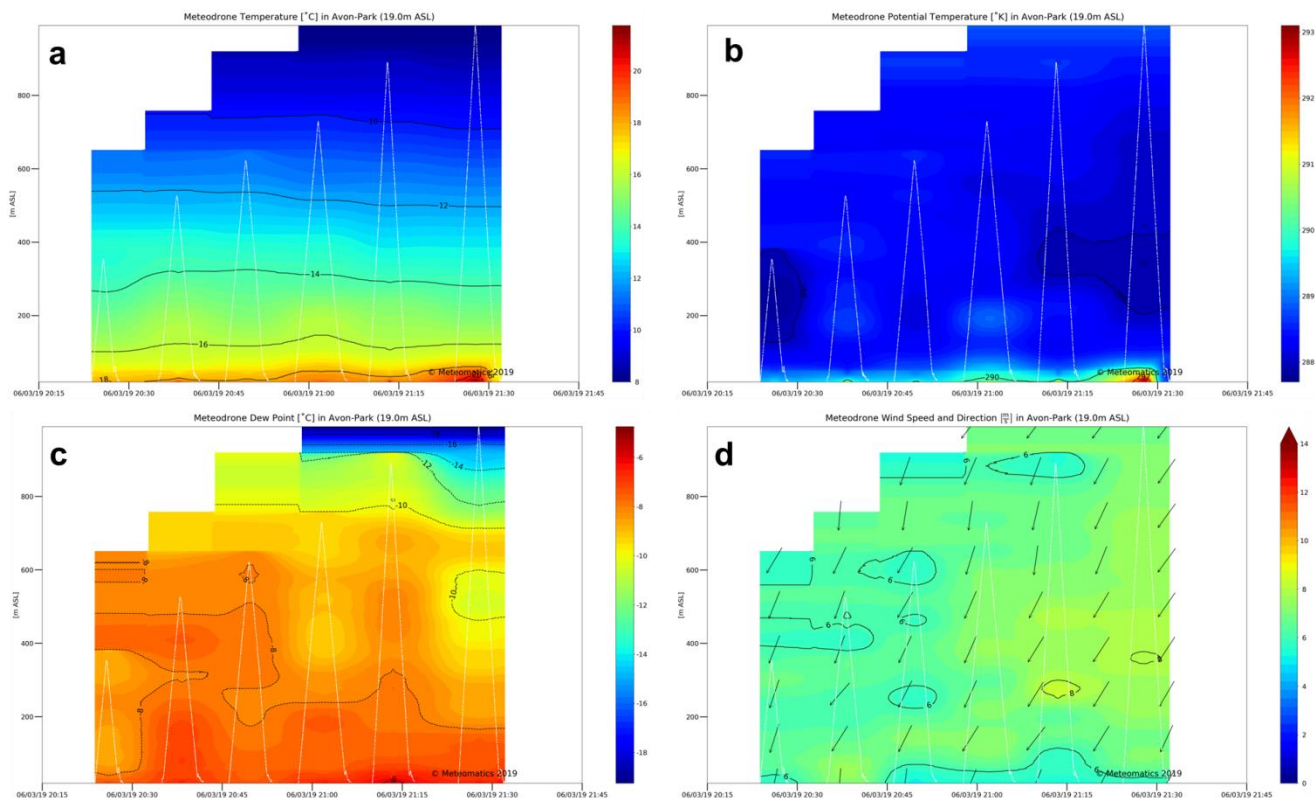


**Figure 6:** Examples of the type of information obtained from the Meteomatics SSE. Panels (a), (b), (c), and (d) show the evolution of temperature, potential temperature, dew point temperature, and wind, respectively, between 20:15 and 21:30 UTC. White lines in each plot show the six sUAS profiles; shading shows the interpolated meteorological fields.

### 3.3. BST S2 Flights

The BST S2 flights provided additional characterizations of the spatiotemporal variability in temperature and moisture fields. As discussed in Section 2, during the flights on 6 March, the BST S2 was flown in a series of lawnmower-type flight patterns. During the first flight, between 19:03 and 19:37 UTC, the lawnmower flights from the BST S2 were at a constant altitude of 350

m AGL, before the BST S2 descended to 250 m AGL (Figure 7). In the second flight, between 20:32 and 21:07, the BST S2 was flown at constant heights of 350 m, 250 m, and 150 m AGL (Figure 8).

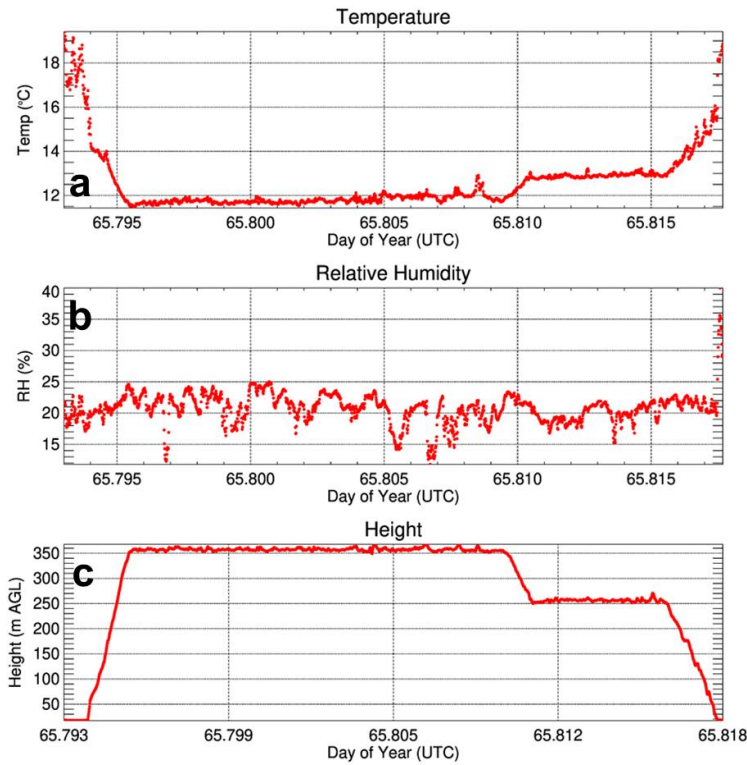


**Figure 7:** Temperature (a), humidity (b), and height AGL (c) during the BST S2 flight on 6 March 2019 between 19:03 and 19:37 UTC.

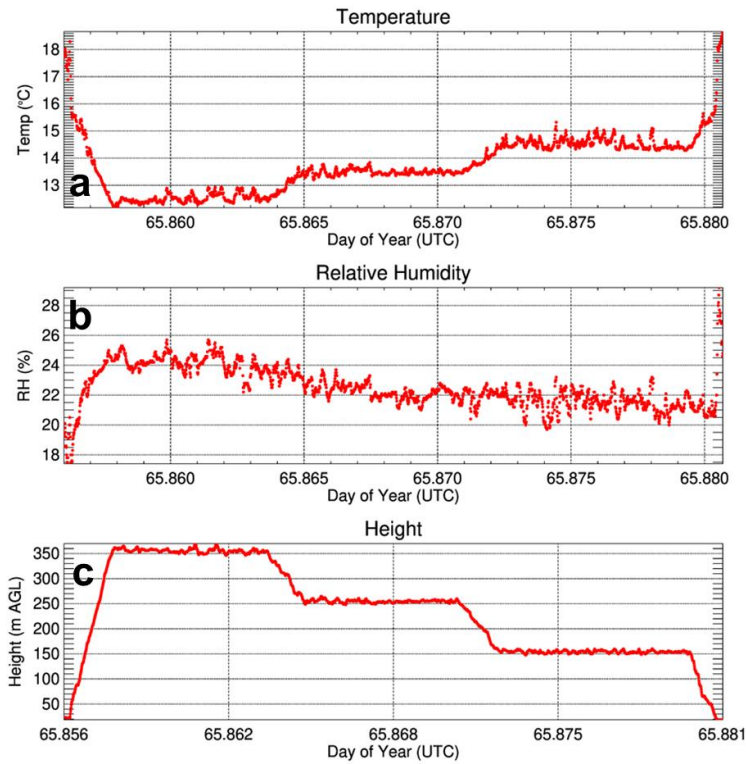


**Figure 8:** Temperature (a), humidity (b), and height AGL (c) during the BST S2 flight on 6 March 2019 between 20:32 and 21:07 UTC.

These lawnmower flights allowed us to map out spatial variations over a  $\sim 1 \text{ km} \times 1 \text{ km}$  box surrounding the launch site. Multiple flights over the same area at a fixed altitude, as shown in the example from 6 March 2019 when the BST S2 was flown at 350 m AGL, show the evolution of ABL temperature and dew point temperature fields (Figure 9). Having this type of information helps quantify the uncertainty and representativeness of point measurements (e.g., those from meteorological towers), which may be useful for the initialization and evaluation of numerical models.

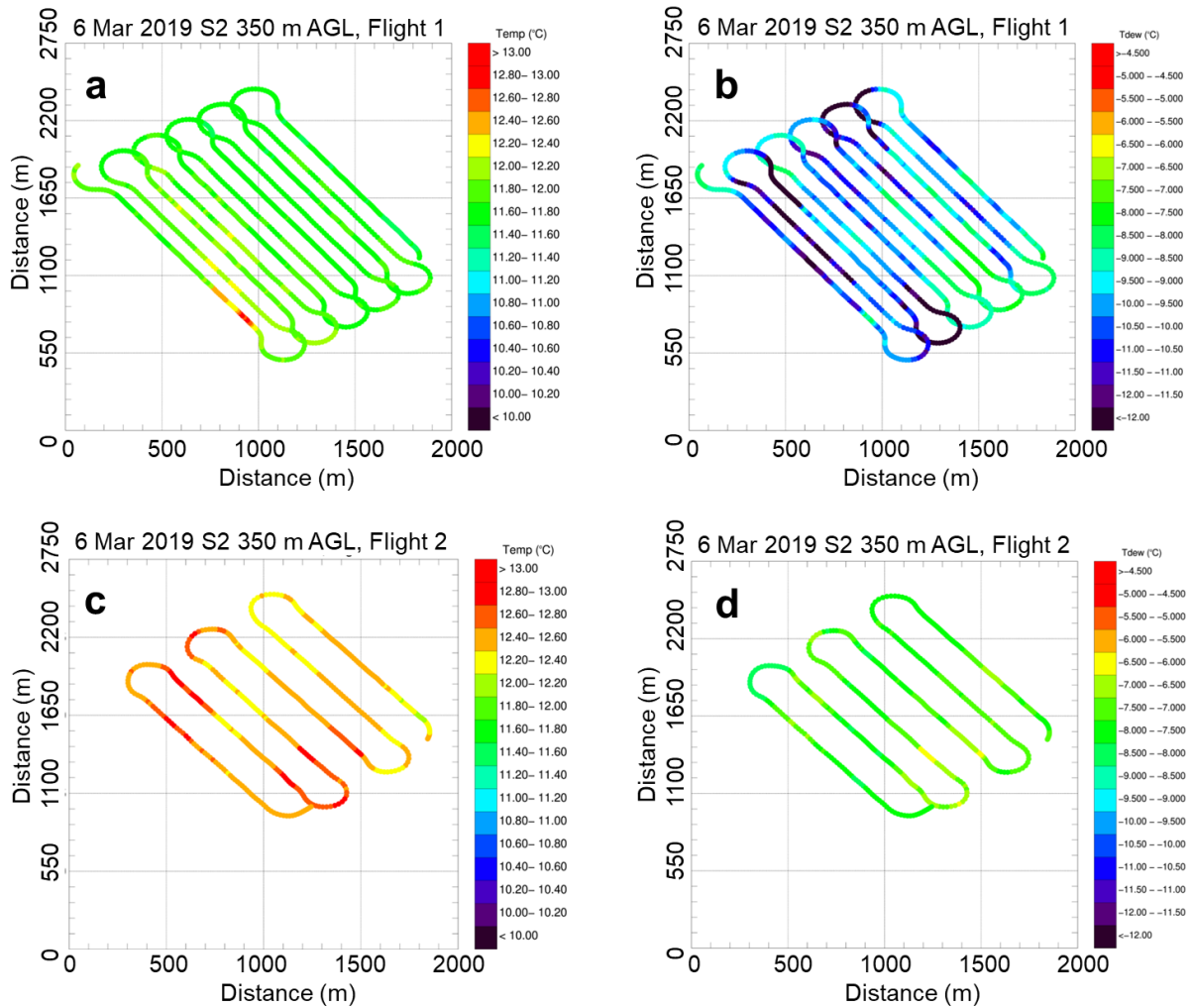


**Figure 9:** In-situ measurements of temperature (a) and dew point temperature (b) between 19:03 and 19:37 UTC 6 March 2019 from the iMet-XQ2 sensor installed on the BST S2 when the BST S2 was flown 350 m AGL. Same for (c) and (d), but between 20:32 and 21:07 UTC 6 March 2019.

The downward-pointing camera installed on the BST provided additional details on thermal characteristics of the land surface. For example, in the images from the lawnmower flights with the BST S2 on 6 March, we found variations in land surface temperature exceeding

10°C over scales of a few hundred meters (Figure 10). These fine-scale gradients are well-known and are consistent with previous work using downward-pointing infrared cameras installed on sUAS during recent field studies (Lee et al., 2019).

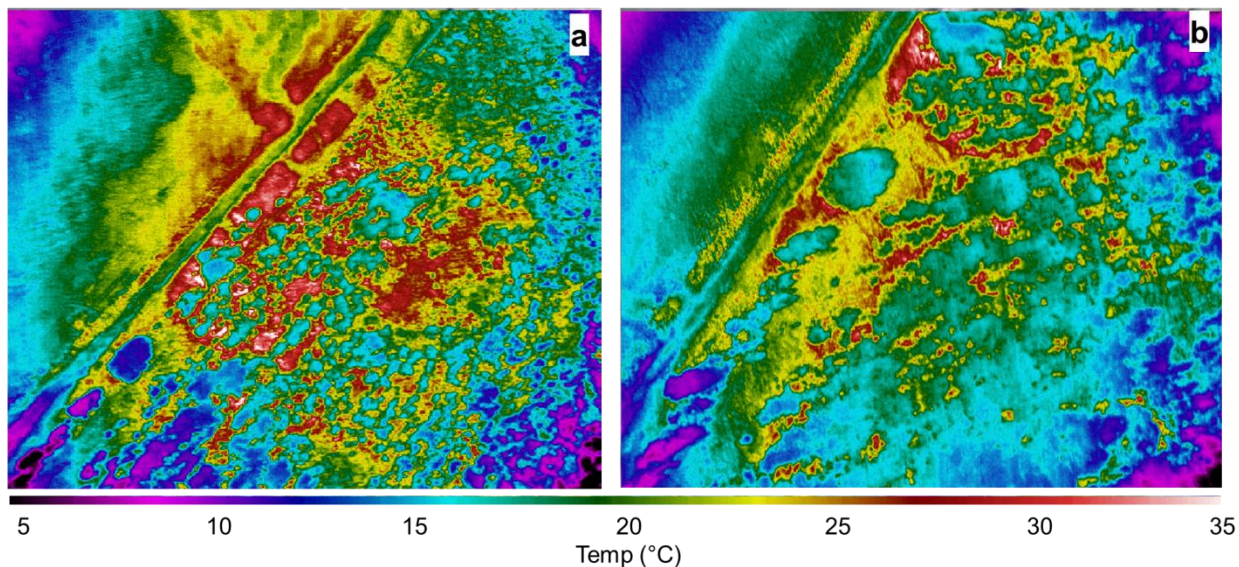


**Figure 10:** Sample images from the downward-pointing infrared camera during the BST S2 flight on 6 Mar 2019 between 19:03 and 19:37 UTC (a) and between 20:32 and 21:07 UTC (b).

### 3.4. Evaluation of Detect and Avoid Systems

During all tests over the period 4-5 March at Avon Park, the ground-based radar system was able to detect both the Meteodrone SSE and BST S2, as well as other air traffic in the area. To help evaluate the ground-based radar system, on 5 March a Twin Otter aircraft from NOAA/OMAO/AOC performed multiple flyovers of the site at select altitudes. The ground-based radar system was able to detect the Twin Otter aircraft, as shown in Figure 11 and Figure 12 from the Kongsberg Geospatial feed and from the Echodyne feed, respectively. Furthermore, the BST S2 was detectable to the unaided eye during all flights, even during the flight when it was flown to its maximum altitude of 1200 m AGL. In contrast, the Meteodrone SSE was visible



only up to ~ 600 m AGL. However, the ground-based radar system was able to detect both of these targets, as shown in the example from 20:30 UTC 5 March 2019 (Figure 13). Overall, Echodyne was able to detect Meteodrone SSE out to around 750-750 m and was able to detect the BST S2 out to a maximum range of 900-1100 m. These tests provide us with confidence in the ability of the Echodyne and Kongsberg systems to help deconflict the airspace in which the sUASs operate.

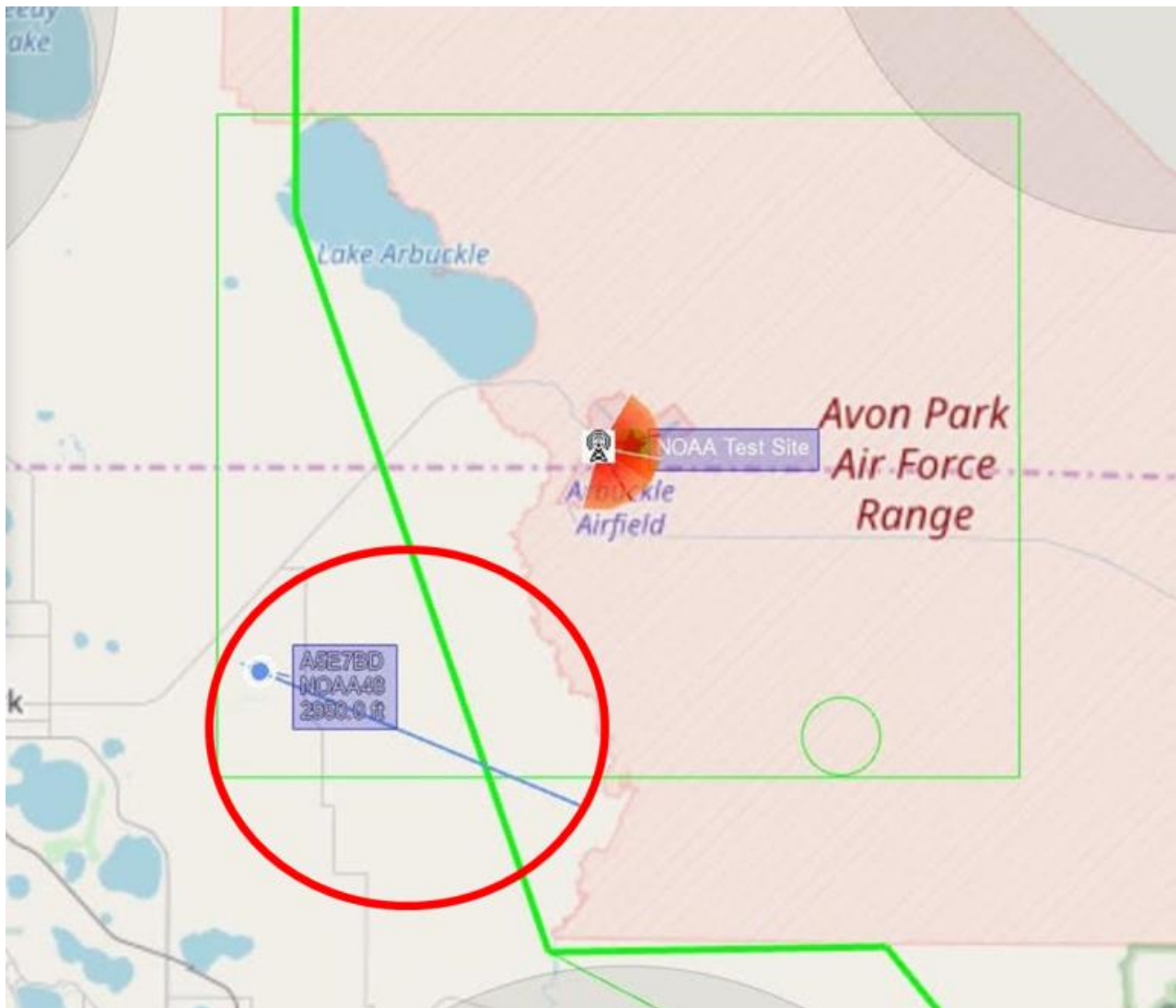


**Figure 11:** Kongsberg Geospatial software detecting the NOAA Twin Otter Aircraft (circled) during its approach to Avon Park, FL.



**Figure 12:** Echodyne software detecting the BST S2 (left target) and NOAA Twin Otter Aircraft (right target). Image taken at 14:08 UTC (panel a) and 14:12 UTC (panel b) 5 March 2019.



**Figure 13:** Echodyne software detecting the BST S2 (left target) and Meteodrone SSE (right target). Image taken at 20:30 UTC 5 March 2019.

## 4. Summary and Outlook

The work at Avon Park was a critical step toward flying sUAS to higher altitudes to assist in weather forecasting applications. To this end, NOAA's AOC and UASPO are working toward obtaining Certificates of Authorization (COA) from the FAA to fly these aircraft up to 3500 ft AGL. Once COAs are obtained, both of ATDD's sUASs will be used for vertical profile sampling within the lowest 1 km of the atmosphere. Higher altitude, more frequent measurements will greatly enhance future field intensive studies of the PBL. Although the BST S2 used in the present study was outfitted only with sensors to measure temperature and moisture in-situ, as well as land surface temperature, the BST S2 can be outfitted with additional instrumentation which ATDD has acquired to obtain additional PBL measurements. This instrumentation includes a multi-hole probe for calculating  $u$ -,  $v$ -, and  $w$ -wind components to derive momentum fluxes, a fast-response temperature humidity sensor for deriving sensible and latent heat flux, a fast-response sensor to measure carbon dioxide and methane concentrations, an airborne lidar for land surface characterization, and a multi-spectral camera to sample surface radiation at select wavelengths. Flying at higher altitudes will help increase the measurements' footprint, potentially making the data obtained from sUAS more useful to numerical modeling applications.

Flying sUAS to higher altitudes than are presently possible in the NAS should also be of significant benefit to operational weather forecasting by the NWS. To support this work, in spring 2019, ATDD will begin flying its Meteodrone SSE up to 1 km AGL to sample vertical profiles of ABL temperature, moisture, and wind. This information will be provided to the weather forecast office (WFO) nearest ATDD, located in Morristown, TN, in real-time to facilitate decisions about short-term weather forecasts. ATDD will also continue working with

AOC and UASPO to obtain FAA COAs to fly the sUAS to ~ 3 km AGL (~ 10,000 ft AGL) to sample within and above the PBL.

The ultimate goal of this work will be to perform the vertical sUAS profiles in an autonomous or semi-autonomous mode at different locations around the US at altitudes beyond 3 km AGL. As the Morristown weather forecast office (WFO) benefits from having additional, real-time information on ABL thermodynamic and kinematic fields, our goal is that this work will be up-scaled across the NOAA operational community. We envision that sUASs will become an asset at WFOs around the US and that sUAS observations will not only be used operationally by weather forecasters to assist in making forecast decisions, but will also be assimilated in real-time into operational weather forecast models used by the NWS (e.g., the High-Resolution Rapid Refresh (HRRR), North American Model (NAM), etc.). Doing so will augment existing rawinsonde observations that are currently released twice-daily at about 100 NWS offices. The use of sUAS observations by forecasters, and the assimilation of sUAS observations into operational forecast models, should lead to improved weather forecasts.

## **Acknowledgements**

We thank Dr. Rick Saylor of NOAA/ARL/ATDD whose comments and suggestions help improve an earlier draft of the technical memorandum.

## References

- Ágústsson, H., H. Ólafsson, M. O. Jonassen, and Ó Rögnvaldsson, 2014: The impact of assimilating data from a remotely piloted aircraft on simulations of weak-wind orographic flow. *Tellus A*, **66**, 25421, doi:10.3402/tellusa.v66.25421.
- Bourgouin, P., 2000 A method to determine precipitation types. *Weather Forecast.*, **15**, 583–592, doi:10.1175/1520-0434(2000)015<0583:AMTDPT>2.0.CO;2.
- Buban, M. S., T. R. Lee, E. J. Dumas, C. B. Baker, and M. Heuer, 2019: Observations of the effects of a total solar eclipse on surface and atmospheric boundary layer evolution. *Bound.-Lay. Meteorol.*, **2019**, 1-14, doi:10.1007/s10546-018-00421-4.
- Flagg, D. D., and Coauthors, 2018: On the impact of unmanned aerial System observations on numerical weather prediction in the coastal zone. *Mon. Weather Rev.*, **146**, 599–622, doi:10.1175/MWR-D-17-0028.1.
- Hardesty, R. M., and R. M. Hoff, 2012: Thermodynamic Profiling Technologies Workshop Report to the National Science Foundation and the National Weather Service; Technical Report NCAR/TN-488+STR; National Center for Atmospheric Research: Boulder, CO, USA.
- Jonassen, M. O., H. Ólafsson, H. Ágústsson, Ó. Rögnvaldsson, and J. Reuder, 2012: Improving high-resolution numerical weather simulations by assimilating data from an unmanned aerial system. *Mon. Weather Rev.*, **140**, 3734–3756, doi:10.1175/MWR-D-11-00344.1.
- Lee, T. R., M. Buban, E. Dumas, and C. B. Baker, 2017: A new technique to estimate sensible heat fluxes around micrometeorological towers using small unmanned aircraft systems. *J. Atmos. Ocean. Technol.*, **34** (9), 2103-2112, doi:10.1175/JTECH-D-17-0065.1.

- Lee, T. R., M. Buban, M. A. Palecki, R. D. Leeper, H. J. Diamond, E. Dumas, T. P. Meyers, and C. B. Baker, 2018: Great American Eclipse data may fine-tune weather forecasts. *Eos*, **99** (11), 19-22.
- Lee, T. R., M. Buban, E. Dumas, and C. B. Baker, 2019: On the use of rotary-wing aircraft to sample near-surface thermodynamic fields: results from recent field campaigns. *Sensors*, **19** (1), 10, doi:10.3390/s19010010.
- Lundquist, J. K., and Coauthors, 2017: Assessing state-of-the-art capabilities for probing the atmospheric boundary layer: The XPIA field campaign. *Bull. Am. Meteorol. Soc.*, **98**, 289–314, doi:10.1175/BAMS-D-15-00151.1.
- Thériault, J. M., R. E. Stewart, J. A. Milbrandt, and M. K. Yau, 2006: On the simulation of winter precipitation types. *J. Geophys. Res. Atmos.*, **111**, D18, doi:10.1029/2005JD006665.
- Wulfmeyer, V., and Coauthors, 2016: Determination of convective boundary layer entrainment fluxes, dissipation rates, and the molecular destruction of variances: Theoretical description and a strategy for its confirmation with a novel lidar system synergy. *J. Atmos. Sci.*, **73**, 667–692, doi:10.1175/JAS-D-14-0392.1.